PHYSOR 2002, Seoul, Korea, October 7-10, 2002

FIRST MUSE-4 EXPERIMENTAL RESULTS BASED ON TIME SERIES ANALYSIS

C. JAMMES and G. PERRET
Commissariat à l'Energie Atomique
Centre de Cadarache
DEN/DER/SPEX/LPE
13108 Saint Paul-Lez-Durance - FRANCE
cjammes@cea.fr ; gregory.perret@cea.fr

G. IMEL
Argonne National Laboratory
P.O. Box 2528
Idaho Falls, ID, USA 83403
imel@anl.gov

On behalf of the European Community MUSE-4 collaboration.

Abstract

The MUSE-4 experimental program is dedicated to investigating the physical aspects of the so-called accelerator-driven sub-critical systems using the novel coupling of the zero-power fast reactor MASURCA and the high intensity and pulsed-neutron generator GENEPI. This paper describes a part of our recent effort to infer kinetic parameters that are of a high interest for safety and operation purposes. One focuses on dynamic experimental methods based on the reactor kinetics and neutron-noise theory using time series data. A specific acquisition system NIKO has been developed in order to achieve our objective.

1 INTRODUCTION

One major objective of needing experimental data to support an accelerator driven sub-critical system (ADS) is to develop and qualify methods of reactivity measurement and monitoring. In a sub-critical system, the reactivity is one of the most important safety-related parameters because it is directly proportional to the power for a given current and source importance. It seems likely that any regulatory body will demand that the physics of sub-critical reactivity monitoring in a commercial ADS are well understood, and the methods are qualified before considering a license for such a system.

The MUSE (multiplication with an external source) series of experiments being performed at the Cadarache Centre of CEA in France are providing an environment for contributing to this objective [1]. In this paper, we are concentrating on the testing and qualification of methods of measuring and monitoring sub-critical reactivities. Other papers at this conference will present other data contributing to code qualification [2].

We are presenting results obtained from dynamic measurements of reactivity—that is, the inference of reactivity from the analysis of a dynamic or time-dependent signal. We have developed a new data acquisition system for MUSE called NIKO (Neutron tIme markiNg acquisitiOn), which is essentially computer (PC) instrumentation that records the timing of all neutron events, allowing subsequent data analysis after the experiment is over. The time-series-based techniques that we are investigating are the inverse kinetics method, the pulsed neutron source method, the Rossi-α method, and the Feynman-α method. In these dynamic techniques, one makes use of the fact that kinetic behavior in a reactor is related to the reactivity. However, each method is a little different in terms of sensitivity to other parameters such as background fission rate, detector efficiencies, or kinetic parameters such as the delayed neutron constants. We will present analyses of these methods using data from MUSE.

2 INSTRUMENTATION AND ACQUISITION SYSTEMS

In the present MUSE-4 experimental program, the reactor is loaded with MOX fuel, and a deuterium or tritium target is placed in the center, surrounded by a lead buffer. A beam of deuterons strikes the target, and D-D or D-T neutrons are produced. The neutron generator, named GENEPI (Generator of Intense Pulsed Neutrons), is capable of producing about 1×10^6 neutrons/pulse in D-T, and up to 5000 pulses/second. The frequency of GENEPI is variable, from 50 Hz to the maximum of 5000 Hz.

Two configurations have been investigated to date: the critical reference and the sub-critical SC0 ($k \approx 0.995$). Figure 1 displays a schematic view of the MUSE-4 core. Detectors used are 1-mg U235-fission chambers (monitors A to H). From one measurement to another, the multiplication factor k is changed by moving the pilot rod (near monitor F) and the control rod.

2.1 THE STANDARD INSTRUMENTATION AND ACQUISITION SYSTEM AT MASURCA

Standard instrumentation at MASURCA is composed of Multi-Channel Scaler and Pulse Height Analyser cards to investigate the dynamic or static counting rate for classical measurements (e.g. rod-drop, source multiplication, axial and radial reaction rate distributions and spectral indices). Recently, the SAM system [3] has been set up to perform simple and reproductible parallel measurements on all standard MASURCA monitors.

2.2 NIKO: A NOVEL NEUTRONIC TIMEMARKING ACQUISITION SYSTEM

The rationale of the NIKO project has been to provide us with means of performing various analytical techniques using one data set when possible. In other words,

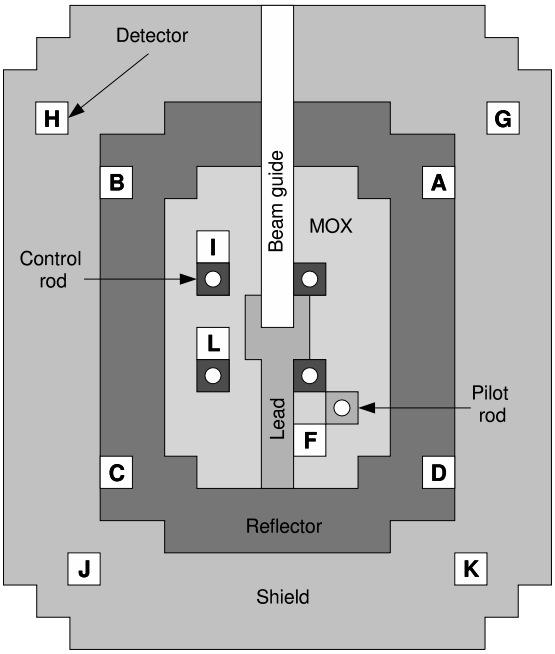

Figure 1. Schematic view of the MUSE-4 core

one seeks the ability to replay neutronic experiments off-line. For that purpose, one needs an aquisition system for timing any events such as counts outgoing from detectors operated in pulse mode. No events are pre-selected by the use of any kind of triggering analog electronics. References [4, 5, 6, 7] describe similar no-trigger instrumentation successfully employed for neutronic experiments and more particuliarly those concerning coincidence techniques.

The main part of our timemarking acquisition system is the MEDaS PC-card designed by the CESIGMA Company. Unlike most similar devices, this acquisition card records the elapsed time between TTL pulses coming into any one of its 32 input channels. Using a clock of 40 MHz, the time resolution is quite high: the dwell time can be fixed at a minimum of 25 ns. That time quantization is compatible not only with the fission chain characteritic time, which is about 200 μs at delayed critical in a fast neutronic system, but also with the dead time of the U235-fission chambers, which is about 50 ns. That somewhat small dead time comes from the fact that the fission chambers are operated in pulse mode with current-sensitive amplifiers.

For any incoming TTL pulse, a pair of 32-bit words is first stored in the internal first-in-first-out (FIFO) memory associated with a 33-MHz PCI bus. The first binary word carries the elasped time from the last event while each bit of the second word is set to 1 in case when the corresponding input channel has detected a TTL signal. With the 33-MHz and 32-bit PCI bus, the MEDaS card makes possible an

acquition rate up to 10 millions events/second.

In order to sustain a satisfying acquisition rate, the features of the host PC is of high importance. For that reason, our acquisition PC is a 800-MHz bi-processor PC whose one processor is dedicated to the PCI bus of the timemarking card. Through the dynamic memory access (DMA) of the host PC, data that are read out from the card FIFO memory are either stored into the random access memory (RAM) or into the hard disk memory when the counting rate is not too high.

3 NEUTRONIC METHODS BASED ON TIME SERIES ANALYSIS

One major objective of the MUSE-4 project is to estimate the following kinetic parameters: the reactivity ρ, the effective neutron delayed fraction β and the generation time Λ. We are interested in the experimental inference of the prompt neutron decay β/Λ at delayed critical and the subsequent inferences of reactivities at below delayed critical. In order to achieve our goal, we have used two kinds of different experimental routes. First, we have estimated different sub-critical reactivities using the inverse kinetics method coupled with the source multiplication method when necessary. Second, we have estimated the prompt neutron decay constant $\alpha = (\beta - \rho)/\Lambda$ for several sub-critical levels using neutron noise techniques. With the exception of the source multiplication method, those techniques are based on experimental time series data.

3.1 INVERSE KINETICS AND SOURCE MULTIPLICATION METHOD

Inverse kinetics is a common method to assess the absolute reactivity level or absolute reactivity worth (absorber, rod worth...). The point kinetic model with 6 delayed groups is used for rod-drop experiments to determine a reference reactivity level. We then use that reference level for determination of other sub-critical states by source multiplication techniques. Spatial effects can be ignored for small reactivity changes less than 1 dollar [8].

In the MASURCA facility, the effective intrinsic source from the MOX fuel is important enough not to be neglected. Starting from a stationnary state (often near criticality) and introducing the detector efficiency ϵ (constant in the point model) we obtain:

$$\rho_{\$}(t) = 1 + \Lambda^* \frac{\dot{c}(t)}{c(t)} - \Lambda^* \frac{\epsilon \bar{Q}(t)}{c(t)} - \sum_j \alpha_j \frac{c(0)}{c(t)} e^{-\lambda_j t} - \sum_j \lambda_j \alpha_j \int_0^t \frac{c(u)}{c(t)} e^{-\lambda_j (t-u)} du \quad (1)$$

where $c(t)$ is the time-dependent counting rate, $\alpha_j = \beta_j/\beta$, $\Lambda^* = \Lambda/\beta$, $\bar{Q}$ the effective source and the other notations are standard. Effective parameters such as Λ, β are pre-calculated with the ERANOS code system using a 33 groups and RZ-geometry [2].

In fact, the source term $S = \Lambda^* \epsilon \bar{Q}/c$ is unknown. We assume that the reactivity is constant after the drop given that the geometry is fixed (i.e. the rod is down). The source term S is deduced by a linear fit after the drop such that a constant reactivity is obtained from Eq. 1 (see Fig. 2). In order to proceed correctly, we have to determine accurately the fitting range to adjust the source term. This is done using statistical tools such as the Durbin-Watson test and residual analyses as well as rod position indicators that give the arrival time of the rod. Uncertainties linked to

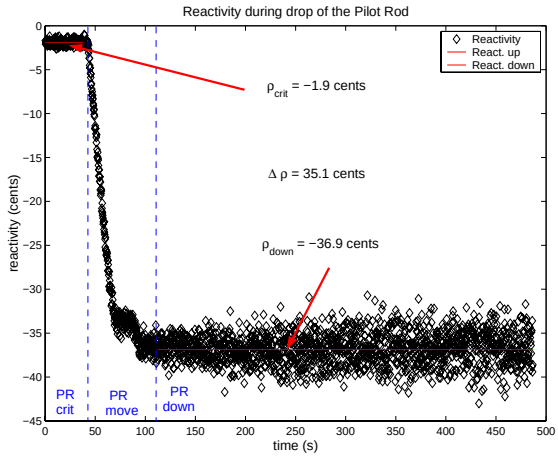

Figure 2. Rod-drop of pilot rod from near critical state to down

reactivity determination by inverse kinetics could be (a) statistical uncertainties on counting rates, (b) fitting uncertainties due to the source adjustment and (c) bias on neutronic constants (e.g. delayed neutron fractions, generation time) and the point model approximation. Uncertainties on counting rates (a) are determined by re-sampling techniques to simulate possible experimental data sets by using for each count c_i of the original set a random number generated from a Poisson distribution around the count c_i. New simulated counting sets provide new reactivities using the same inverse kinetic procedure and so a mean reactivity and a standard deviation. The bias due to neutronic constants (c) is unknown and generally overestimated by an independant 5% value [9].

The reference reactivity level is further used to find out reactivity levels of different configurations by static Source Multiplication (SM) or Modified Source Multiplication (MSM) techniques. With C_0 and C_1 the counting rates for the unperturbed and perturbed levels and ρ_0 and ρ_1 the corresponding reactivity levels we used the MSM formula:

$$\rho_1 = \rho_0 f_{01} \frac{C_0}{C_1} \qquad f_{01} = \frac{\epsilon_1 \bar{Q}_1}{\epsilon_0 \bar{Q}_0} \tag{2}$$

where f_{01} is the MSM correction factor from state "0" to "1" which accounts for the fact that detector efficency ϵ and effective neutron source $\bar{Q}$ may change in going from state "0" to "1". For small reactivity changes ($\lesssim$ \$1) we assume $f_{01} = 1$ (simple SM technique). Statistical uncertainties on ρ_1 are a combination of those of the reference level and the counting rates. The uncertainties on the MSM factor are estimated to 3% and we add a 5% error due to kinetic constants.

3.2 PULSED NEUTRON SOURCE METHOD

The one-group point kinetic model of a reactor predicts that the time dependence of the neutron flux after a pulse of neutrons is injected is:

$$f(t) = \frac{1}{\beta - \rho}\left(\beta \exp^{-\lambda' t} - \rho \exp^{-\alpha t}\right) \tag{3}$$

In this expression, $\lambda' = \rho\lambda/(\rho - \beta)$ and the other notations are standards (see Sect. 3). In most cases of interest, GENEPI is operated at some frequency, and multiple pulses are added to form a time response as if one very large pulse were produced. As the lowest frequency of GENEPI is 50 Hz, this provides a simplification of the above relation, since for all cases of interest then, we can make the assumption that $\lambda' t \ll 1$. This yields an approximation:

$$f(t) = \frac{1}{\beta - \rho}\left(\beta - \rho \exp^{-\alpha t}\right) \tag{4}$$

Thus, the delayed neutrons only provide a constant (with time) source of background. This background must be identified, and correctly subtracted before the slope of the prompt decay α can be identified from experimental data.

In actual fact, there are at least three or four distinct time regimes shown by experimental data. First, we have the rapid buildup and equally rapid decay of the source neutrons, before a prompt fission neutron distribution is stabilized. Then, we have the prompt fission neutron decay, which yields the time constant α that is the objective. However, this can be contaminated by space/energy effects such as moderation of neutrons in the reflector. As the neutrons moderate, detector efficiency increases as a function of time. This will lead to a contribution to the time dependence not given by the above relation. In the last part of the data, we see the pulse begin to approach a background level—whether the constant background is attained or not depends on the frequency of the pulses and the slope of the decay (which in turn depends on reactivity). Typically as the background is approached, the statistics become very poor, especially for low reactivities. This can necessitate very long acquisition times. It is useful to keep the above points in mind as one examines and attempts to analyse the data.

Figure 3 illustrates the decrease of the pulse in the beginning and the approach to the background value at the end of the PNS curve. From the previous remarks we saw that the fit of the PNS curves are sensitive to the fitting domain and the background determination (see Fig. 3). To find the background we can either determine it by fitting the tail of the PNS curve to a constant and use a linear model to fit the logarithm of the reduced data or make it a parameter of a non-linear fit. We have found that the latter generally gives a better estimate of the true background. In order to find the fitting domain, we used statistical tools. The determination of the lower bound is made using an analysis of the residuals and especially the Durbin-Watson test [10] to check the independance of the residuals. This is a clear means to reject any contribution due to GENEPI's pulse decay (see Fig. 4). This operation is one of the most important for the fit accuracy. The upper bound is determined by the maximization of the correlation coefficient referred to as the R-value in Fig. 5. This statistic allows us to evaluate the goodness of fit. This criteria

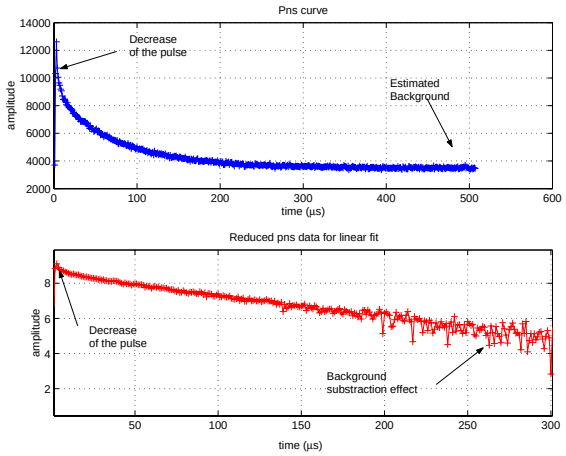

Figure 3. PNS curve - Raw and reduced data

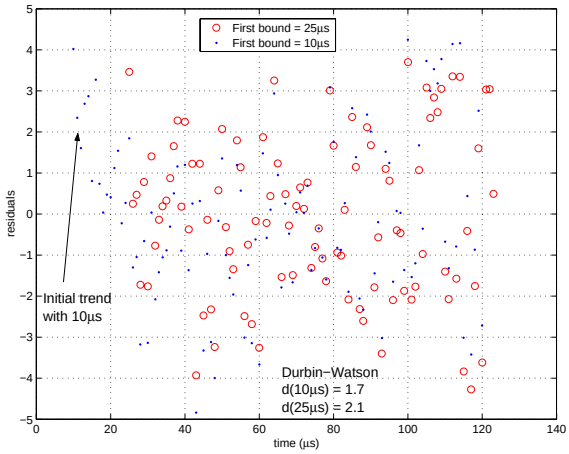

Figure 4. Residuals and the Durbin-Watson test

is an approximation in the sense that the R-value often stay close to one over a large range. It is however appropriate since the fit is not too sensitive to the upper bound.

The uncertainties linked to the fitted α-value are due (a) to the fitting techniques and (b) to the correct choice of the bounds. The first is correctly determined if the residuals are independant (Durbin-Watson test) and normally distributed around zero (Kolmogorov-Smirnov test). The fitting uncertainties are of type A [11] and are well characterized by a standard deviation σ. The uncertainties linked to range determination are more empirical and are based on the spread of α resulting from bounds changes. This is a type-B uncertainties [11]. As the underlying process is unknown, constant statistical law is assumed and we propose the following expression for type-B uncertainties, which is a measure of spread:

$$\delta = \frac{\alpha_{max} - \alpha_{min}}{2} \tag{5}$$

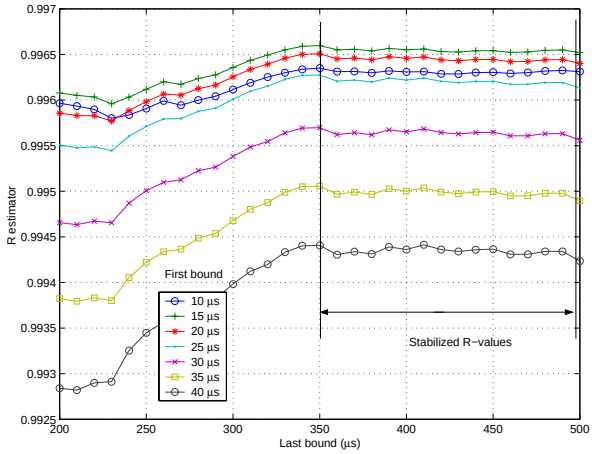

Figure 5. Non-linear fitting and the R-test

3.3 ROSSI-α METHOD

The well-known Rossi-α technique [12] is based on the statistical nature of the fission-chain process. Using a coincidence acquisition system, the rationale is to experimentally determine the probability distribution of detecting neutrons from the same chain. The Rossi distribution, related to the correlation function of neutron detection time series, can be derived theoritically through a birth-to-death probability balance equation, namely the backward master equation [13] . In this paper, we only consider the following Rossi distribution p_{rossi} for a point kinetic model without delayed neutrons:

$$p_{rossi}(\tau)dt_g dt_c = \epsilon_g F_0 dt_g(\epsilon_c F_0 dt_c + \frac{\epsilon_c D}{2\alpha\Lambda^2} dt_c e^{-\alpha\tau}), \quad \tau = t_c - t_g \tag{6}$$

The above expression can be heuristically derived. The Rossi-α experiment is as follows. There are two input channels: a trigger channel with detection efficiency ϵ_g and counting channel with efficiency ϵ_c. Those two channels can be provided by either a single detector (auto-correlation) or two seperate detectors (cross-correlation). A time gate ΔT divided in bins of width δt_c is opened at a certain time t_g by a pulse from the trigger channel. Some bins δt_c corresponding to the elapsed time between the occurence of a pulse from the counting channel at t_c and this of the original trigger pulse are then incremented. Since a timemarking acquisition system is capable of recording all the events of any detector and thus makes possible an offline data reduction, a time gate of width ΔT is opened for each trigger pulse. This data processing is reffered as to the Rossi-α type I in the literature.

According to Eq. 6, the number of coincidence counts n_{rossi} in a bin i corresponding to the lag $\tau = i\delta t_c$ is given by:

$$n_{rossi}(\tau) = n_{rand} + n_{corr} e^{-\alpha\tau} \tag{7}$$

The uncorrelated or random component n_{rand} is:

$$n_{rand} = N_g \epsilon_c F_0 \delta t_c \tag{8}$$

where $N_g = \epsilon_{tg} F_0 T$, the number of time gates, is proportional to the acquisition duration T. The correlated component n_{corr} is:

$$n_{corr} = N_g \epsilon_c \frac{D}{2\alpha\Lambda^2} \delta t_c \tag{9}$$

Assuming that the number of coincidence counts n_{rossi} approximately follows a Poisson distribution, its standard deviation $\sigma_{n_{rossi}}$ is:

$$\sigma_{n_{rossi}}(\tau) = \sqrt{n_{rossi}(\tau)} \tag{10}$$

3.4 FEYNMAN-α METHOD

Feynman and de Hoffman [7] showed that the number of counts c in a time gate ΔT deviates from a Poisson distribution because of the fluctuations of the neutron population driven by the fission chain process. For a given time gate ΔT, the deviation is measured by the y-value defined as:

$$y = \frac{variance}{mean} - 1 = \frac{\overline{c^2} - \overline{c}^2}{\overline{c}} - 1 \tag{11}$$

That expression can be generalized to the case of possibly two different detectors k and l with detection efficiencies ϵ_k and ϵ_l, respectively:

$$y_{k,l}(\Delta T) = \frac{\overline{c_k c_l} - \overline{c_k}\,\overline{c_l}}{\sqrt{\overline{c_k}\,\overline{c_l}}} - \delta_{k,l} \tag{12}$$

where $\delta_{k,l}$ is the Kronecker symbol. For $k \neq l$, the numerator of the y-value is a covariance term.

The y-value is related to the Rossi distribution through the average number of pairs counted in a time gate ΔT:

$$\frac{\overline{c_k(c_l - \delta_{k,l})}}{2} = \int_0^{\Delta T} dt_c \int_0^{t_c} dt_g \quad p_{rossi}(t_c - t_g) \tag{13}$$

One thus obtains the following expression for the y-function assuming a point kinetic model and considering prompt neutrons only:

$$y_{k,l}(\Delta T) = \frac{\sqrt{\epsilon_k \epsilon_l} D}{\alpha^2 \Lambda^2} \left(1 - \frac{1 - e^{-\alpha \Delta T}}{\alpha \Delta T} \right) \tag{14}$$

The standard deviation σ_y of the y-value can be approximately derived from those of the sample variance and mean of the normal distribution:

$$\sigma_y = \frac{1 + y_{k,l}}{\sqrt{N}} \sqrt{\frac{1 + y_{k,l}}{m_{k,l}} + 2}, \quad m_{k,l} = \sqrt{\overline{c_k}\,\overline{c_l}} \tag{15}$$

where N is the number of samples (i.e. the number of counts) for a given time gate ΔT.

The y-value can be sometime negative because of either a dead time effect at high counting rates [14] or a poor statistics in a system with neutron generation times Λ less than 10 μs [15]. Assuming a non-paralyzable counting system, Yamane proposed the following improved formula [14]:

$$y^d_{k,l} = y_{k,l} - 2Rd\delta_{k,l} \tag{16}$$

where d and R are the total dead time and the counting rate associated to a neutron channel, respectively.

4 FIRST MUSE-4 EXPERIMENTAL RESULTS

4.1 RESULTS FOR INVERSE KINETICS AND SOURCE MULTIPLICATION METHODS

The reactivity level in the reference configuration is obtained for the pilot rod down and all the control rods up. It is in good agreement among all detectors except F which is close to the pilot rod (see Fig. 1). We can give a reference reactivity level $\rho_{REF} = 36.7 \pm 0.2\,¢$. The conservative independant error applied to take into account the kinetic constants uncertainties is 5% (see Sect. 3.1).

Reactivity level in the SC0 configuration has been determined for 3 rod positions: (a) 4 control rods up and pilot rod up (PRU), (b) 4 control rods up and pilot rod down (PRD) and (c) 1 control rod down and pilot rod down (CRD). We have used inverse kinetics followed by SM/MSM techniques on core monitors F, I and reflector monitors C, D (see Sect. 3.1). Results of Table I show values of different levels with the statistical uncertainties. Good agreement among all detectors has been achieved when all control rods are up. When the control rod is down, spatial effects are significant but MSM corrections reduced the spread $\delta = (\rho_{max} - \rho_{min})/2$ among the monitors to 3.2% which is the order of the uncertainties on each value.

Region	Monitor	ρ (\$) and Std. Error σ_ρ					
		PRU (by SM)		PRD (by SM)		CRD (by MSM)	
Core	F	1.32	1.1%	1.76	1.1%	12.75	3.2%
	I	1.35	1.9%	1.75	0.9%	12.03	3.1%
Reflector	D	1.31	0.4%	1.72	0.5%	12.47	3.0%
	C	1.32	0.5%	1.72	0.5%	12.87	3.0%
ρ/σ		1.33	0.4%	1.74	0.4%	12.53	1.5%

Table I. Subcritical reactivity levels in SC0

4.2 RESULTS FOR PULSED NEUTRON SOURCE METHOD

The pulsed neutron source method has been used with the deuterium target in the configuration SC0 with the aforementioned 3 different rod positions and with frequencies of GENEPI varying from 1 to 4 kHz. U235-fission chambers has been used

in each region of MASURCA: Monitors F and I in the core, A, B, C and D in the reflector and G and H in the shield (see Fig. 1). This allows us to investigate: (a) the influence of the GENEPI frequency, (b) the spatial effects and (c) the reactivity level effects (rod position). The energy-dependent aspects are left for further experiments.

In the theoretical case, the frequency of GENEPI must have no effect on the true value of α. The standard deviation due to frequency $\sigma_{\bar{\alpha}}$ in Table II confirms this assumption in the core and the reflector region within the limits imposed by the uncertainties of type A and B (σ_α and δ). This is obtained thanks to the non-linear fit where background is sufficently well-estimated. A simple linear model would have overestimated the α-value for frequencies greater than 2 kHz in this configuration (see Sect. 3.2). We can also point out from this table the decrease of α from the core region to the reflector and the good agreement of different detectors in the same region. The impact of reactivity level on the fitted α-values are given for the pilot and control rods in Table III. First, the standard deviation $\sigma_{\bar{\alpha}}$ for the mean α value

Freq. (kHz)	α (s^{-1}) and σ_α/δ (%)							
	Core Monitors				Reflector Monitors			
	F		I		A		C	
1	12849	1.6/2.8	12645	1.4/3.7	12397	0.6/1.1	12336	0.6/1.0
2	13123	1.3/1.3	13014	1.0/2.6	12217	0.7/1.4	12314	0.7/1.7
3	13193	1.4/3.4	13484	1.1/2.0	12239	0.7/1.1	12225	0.7/1.5
4	13348	1.5/1.7	13213	1.2/3.0	12123	0.9/1.7	12292	0.8/1.2
$\bar{\alpha}/\sigma_{\bar{\alpha}}$	13128	1.6%	13089	2.7%	12244	0.9%	12292	0.4%

Table II. α-value vs. GENEPI frequency in SC0/PRU

Region	Monitor	α (s^{-1}) and σ_α/δ (%)					
		PRU		PRD		CRD	
Core	F	13269	1.7/3.5	15594	1.2/1.0	63275	1.7/5.4
	I	12767	1.5/3.3	15562	1.5/2.5	64052	2.2/8.6
	$\bar{\alpha}/\sigma_{\bar{\alpha}}$	13018	2.7%	15578	0.1%	63664	0.9%
Reflector	C	12397	0.8/1.0	14265	0.8/2.0	51113	1.2/17.6
	D	12230	0.7/1.1	14263	0.8/1.0	52900	1.0/14.7
	$\bar{\alpha}/\sigma_{\bar{\alpha}}$	12314	1.0%	14264	0.1%	52027	2.4%
Shield	G	11196	1.0/4.4	13009	0.9/3.4	44680	1.5/24.1

Table III. α-value vs. reactivity level

in the core and reflector region is always smaller than the experimental spread on the fit δ. Second, the spread δ increases quickly with the decrease of the reactivity level whereas the fitting uncertainties σ_α stay close to 1-3%. This is probably due

to the difficulty of choosing the correct interval for the fit of α when $k \approx 0.97$. This prevents us from analysing the spatial effects resulting from control rod insertion on monitors F and I (see Fig. 1). The decrease of α-values from the core to the shield region ($\Delta\alpha$) is increased when the reactivity level decrease: $\Delta\alpha = 2569\,s^{-1}$ (equivalent to 60 cents) when the pilot rod is down and $\Delta\alpha = 18984\,s^{-1}$ (1.99 dollars) when the pilot and the control rod is inserted. This can not be explain by the given uncertainties. The following 3 α-values are then deduced from measurements in the core region:

$$\alpha_{PRU} = 13018\,(3.5\%) \quad \alpha_{PRD} = 15578\,(2.5\%) \quad \alpha_{CRD} = 63664\,(8.6\%)$$

where only the maximum type-B spread is considered for uncertainties.

4.3 RESULTS FOR FEYNMAN- AND ROSSI-α METHOD

Noise techniques have been performed for the MUSE-4 reference core (1115 fuel cells) with the pilot rod down. The corresponding reactivity is $\rho_{REF} = 36.7 \pm 0.2\,¢$ (see Sect. 4.1). We are presenting in this section the different α-values obtained with the Rossi- and Feynman-α methods. Eight runs of 2800 s have been done with the acquisition system NIKO. The dwell time has been set to 100 ns. It is important to notice that the most efficient monitors G and H have to be moved to the reflector region for this noise experiment series. The positions of monitors G and H have been thus exchanged with those of monitors A and B, respectively.

The Rossi- and Feynman-α experimental data series are analysed with the use of a least squares fitting method. For evaluating the goodness of fit, one uses graphical and numerical indicators. The scatter plot should not display any pattern. In other words, the residuals that are the differences between the reponse values and the predicted reponse values should be random errors. One uses the standardized residuals that are the ordinary residuals divided by their standrad deviation. The closer to 1 the square of the correlation coefficient r^2 is, the better the fit is. This statistic measures how successful the fit is in explaining the variation of data. The root mean squared error, $RMSE$, is another statistic closely related to the scatter plot since it is defined as the square root of the summed square of residuals divided by degrees of freedom. The $RMSE$ value has to be minimized.

The Rossi-α fitting model is $p(\tau) = n_{rossi}(\tau)/n_{rand}$ (Eq. 7). The domain of fit spans from 10 μs to 1 ms since in the case of cross-coincidence the lag τ is not likely to be less than 10 μs (see Fig 6). Table IV shows the fit results. The detectors C, D, I and F do not allow us to accurately estimate α-values because of low statistics. While for the detectors G and H, the standard errors are about 1%, the discrepancies between α-values are quite large. Their variability can be expressed by the means of the type-B uncertainty proposed in Eq. 5:

$$\alpha_{RA} = \bar{\alpha} \pm \delta = 8017 \pm 673\ \text{s}^{-1} \quad (8.4\%)$$

The Feynman-α fitting model is given by Eq. 14. The domain of fit spans from 0 to

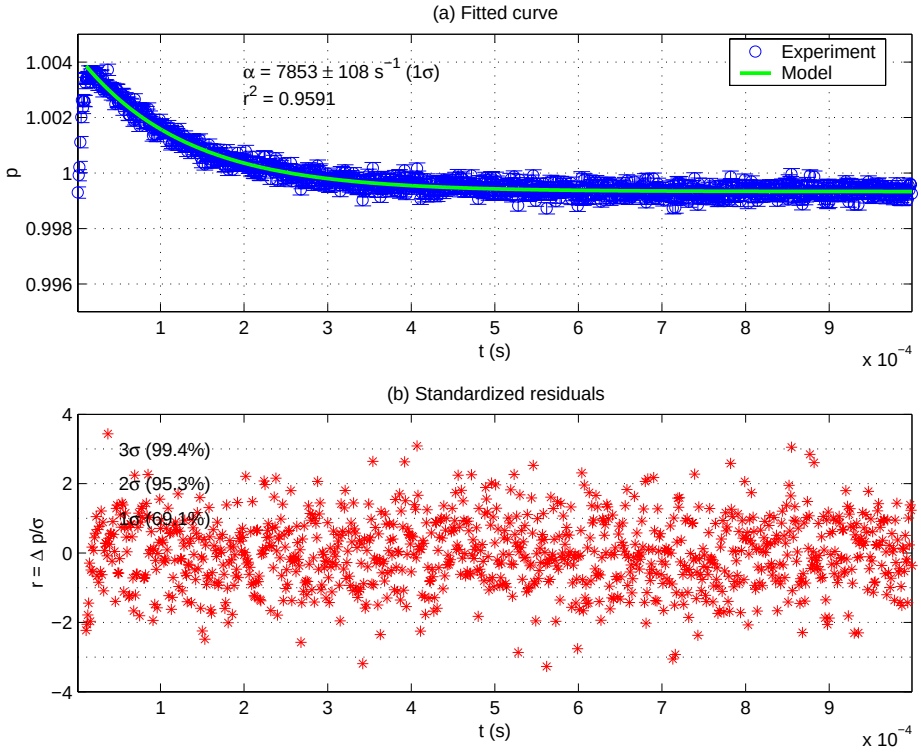

Figure 6. Fit of the Rossi distribution for (H,H) detectors

1 ms. We note that we do not make a dead time correction to the Feynman model because our 5 ns dead time is much less than the minimum 100 ns gate width. On the other hand, it is necessary to add a constant term to the covariance-to-mean model, that is given by Eq. 14 in order to successfully fit the experimental data series. This corrected model that is referred as to the shift correction in Table V has to be investigated with care. Taking account of those two remarks, Table VI shows the fit results. Figure 7 shows the fitted curve obtained with the detector H. The α-estimates obtained with the detectors I and F are rejected because of their poor statistical indicators. For the other detectors, the discrepancies between α-values are quite large even if the standard errors are less than 2%. Their variability is

Region	Monitors	α (s^{-1})	σ_α (%)	r^2	$RMSE$
Reflector	(G,G)	8901	1.1	0.9725	1.0348
	(H,H)	7853	1.4	0.9591	1.0096
	(G,H)	7555	1.2	0.9670	0.9892
	(H,G)	7757	1.2	0.9662	1.0107
Core	(I,F)	7296	49.4	0.0181	1.0228
Reflector	(C,D)	7781	11.2	0.2636	1.0194

Table IV. Fit results for the Rossi-α method

measured in the same manner as the Rossi-α case:

$$\alpha_{FA} = \bar{\alpha} \pm \delta = 8244 \pm 688 \text{ s}^{-1} \quad (8.3\,\%)$$

Shift Correction	α (s^{-1})	σ_α (%)	r^2	$RMSE$
No	18428	6.1	0.9175	12.05
Yes	7850	0.2	0.9999	0.23

Table V. Shift correction for (G,H) detectors

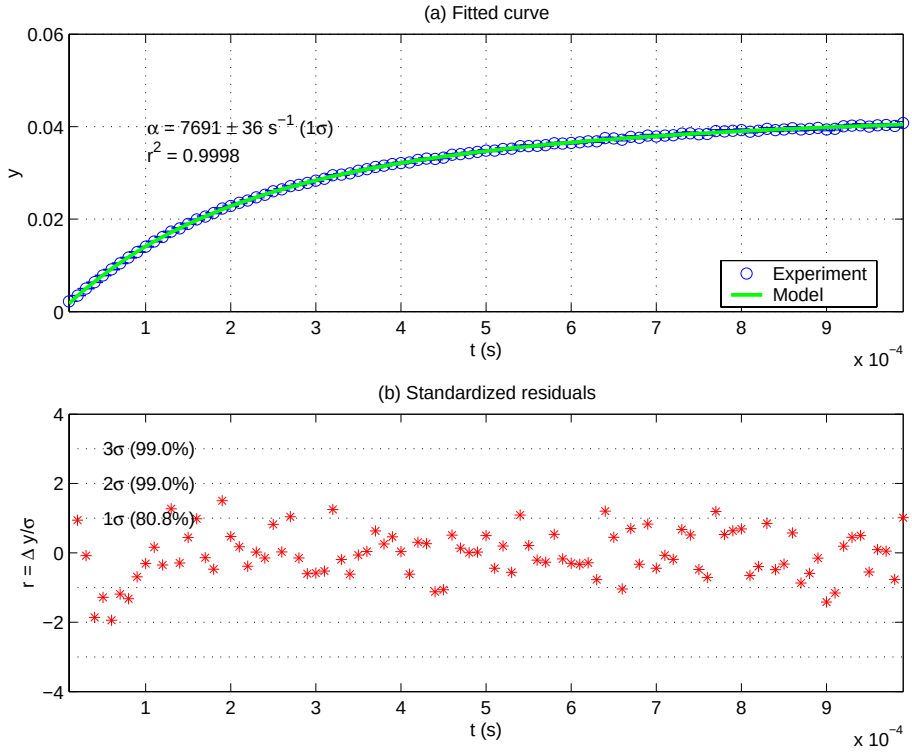

Figure 7. Fit of the y-function for (H,H) detectors

4.4 INTER-COMPARISON

In this paper, we have presented results from MSM (static), inverse kinetics, PNS, and Rossi- and Feynman-α (all dynamic). We now wish to make some preliminary conclusions about these measurements and what we can infer from them.

First, we summarize the various measurements and their configurations in Table VII. We do not display the individual uncertainties in this table, as this is just a table

Region	Monitors	α (s^{-1})	σ_α (%)	r^2	$RMSE$
Reflector	(G,G)	8046	0.5	0.9997	1.62
	(H,H)	7691	0.5	0.9997	1.26
	(G,H)	7850	0.2	0.9999	0.46
Reflector	(C,C)	8917	2.6	0.9882	0.82
	(D,D)	9066	1.6	0.9955	0.54
	(C,D)	7891	1.9	0.9976	0.36
Core	(I,I)	9847	5.9	0.9314	0.82
	(F,F)	8359	7.1	0.9090	0.54
	(I,F)	7045	11.1	0.9243	0.36

Table VI. Fit results for the Feynman-α method

Reference Core		
REF	Inv. Kinetics	$\rho = 0.367$ dollars
	Feynman-α	$\alpha = 8239\ s^{-1}$
	Rossi-α	$\alpha = 8538\ s^{-1}$
SC0 Core		
PRU	MSM	$\rho = 1.33$ dollars
	PNS	$\alpha = 13018\ s^{-1}$
PRD	MSM	$\rho = 1.74$ dollars
	PSN	$\alpha = 15578\ s^{-1}$
CRD	MSM	$\rho = 12.53$ dollars
	PSN	$\alpha = 63664\ s^{-1}$

Table VII. Summary of all measurements

meant to collect and display the various measurements. We begin with the reference reactivity, obtained in the case of the pilot rod down (REF) and the reference core configuration. This reactivity is obtained from inverse kinetics, and can be shown to be insensitive to uncertainties in the delayed neutron parameters when the reactivity is presented in units of dollars. From this point, we then use source multiplication techniques to obtain reactivities in the sub-critical configurations SC0 with the pilot rod up (PRU), down (PRD), and one control rod and pilot rod down (CRD). We can use these reactivities to normalize our dynamic measurements (PNS, Feynman- and Rossi-α) by using them to infer the ratio of β/Λ. This ratio is very important, as it is the rate above which the reactor can no longer significantly respond to perturbations. In general, we can write:

$$\frac{\beta}{\Lambda} = \frac{\alpha}{\rho_\$ - 1} \tag{17}$$

where we specifically note that the reactivity is in units of dollars. We present the infered values of β/Λ in Table VIII. We would assume this ratio to be constant as we change configurations, as we are not changing the geometry or composition of the core greatly[1].

[1]We are in the process of performing more calculations to confirm this.

Configuration	Reactivity ($)	$\beta/\Lambda(s^{-1})$	Uncertainties
Reference Core			
REF Rossi	0.367	5865	8.9%
REF Feynman	0.367	6031	8.3%
SC0 Core			
PRU PNS	1.33	5587	3.5%
PRD PNS	1.75	5665	2.5%
CRD PNS	12.53	4705	8.6%

Table VIII. Inferred β/Λ

For common configurations, such as Rossi vs. Feynman in the reference core, or the measurements at SC0 with pilot rod up or down (only a 40 cent change), there is good agreement among the methods. The agreement is well within the assumed uncertainties. However, there is clearly a trend as the configuration is changed in going from just slightly sub-critical (Reference) to SC0 (maximum of -1.33 dollars), to SC0 with a control rod inserted (-12.53 dollars). The trend is towards a decreasing ratio of inferred β/Λ, and in fact the change is $\sim$20% in going from the reference core to SC0 with one control rod inserted. At the present time, we do not believe that there is a significant change in β/Λ, so it appears that the model of a simple exponential decay after the pulse is deficient, and that the time structure is more complex. One potential explanation is that there is moderation occuring after the pulse, so detector efficiencies are increasing with time. This would have the effect of increasing the apparent generation time, which would decrease the α measured. Note that this apparently is what is happening in the detectors in the shield and reflector—perhaps there is also an effect in the core although it is less. We are still in the process of investigating this phenomenon.

Note that we can take another approach in analyzing the data. First, we can assume that the ratio β/Λ as given by the Rossi- and Feynman-α is the true, and invariant variable. One can then infer the reactivities from Eq. 17. Thus, we will assume that $\beta/\Lambda = 5948\,s^{-1}$. This implies the reactivities given in Table IX. We assume the same uncertainties. We note from Table IX that when reactivity is inferred, we see

Configuration	$\alpha(s^{-1})$	Reactivity ($)	Uncertainties	ΔMSM ($)
Reference Core				
REF Rossi	8017	0.348	8.9%	-0.019 (5.2%)
REF Feynman	8244	0.386	8.3%	+0.019 (5.2%)
SC0 Core				
PRU PNS	13018	1.19	3.5%	-0.14 (10.5%)
PRD PNS	15578	1.62	2.5%	-0.13 (7.4%)
CRD PNS	63664	9.70	8.6%	-2.83 (22.6%)

Table IX. Inferred $\rho_{\$}$

a shift from MSM to the PNS methods of about 13 cents, but the $\Delta\rho$ is constant at about 42 cents. Thus, the worth of the pilot rod is consistently predicted with both methods. Again, when we look at the case of the control rod down in SC0, we see a much greater shift, from 12.53 to 9.70 dollars. This is essentially the same $\sim$20% trend towards underprediction of the α that we have previously discussed. We are continuing to study this problem, and as we take more data at other reactivity levels, we will be able to discuss more on this topic.

5 CONCLUSION

In this paper, we have presented measurements based on the time series data collected in the MUSE-4 experiments. We have used PNS, Rossi- and Feynman-α techniques to infer the ratio β/Λ, a parameter that determines the time scale of kinetic behavior of a reactor system. We have found a fairly large spread (up to 20%) in our determination of this parameter as the system is perturbed by the insertion of a control rod ($k \approx 0.97$). We intend to perform more such measurements to try to better understand this phenomenon.

We see two trends in the α-values (prompt neutron decay constant). As we lower the reactivity of the system, we obtain lower α-values than we would expect (see above paragraph). Additionally, as we move from detectors in the core, to detectors in the reflector, to finally detectors in the shield, we see also a decrease in the α-values. At the present time, we are surmising that this phenomena is due to the slowing-down of neutrons in the reflector and shield regions, which increases the detector efficiency. This has the effect of increasing the *effective* generation time in these outer regions. It is certainly possible to infer reactivity from dynamic measurements of this type. We saw that in the case of PNS, we were able to determine the δk worth of the pilot rod with very good agreement to the MSM techniques. However, the absolute value shows a 10-20% deviation.

These measurements have just begun in the MASURCA facility, and the preliminary results are encouraging. However, we need many more such measurements before we can demonstrate that we can infer the sub-critical reactivity with an uncertainty on the order of 5% or less. By the end of the MUSE-4 program (end of 2003) we will have accumulated the necessary measurements.

6 ACKNOWLEDGEMENTS

We are indebted to Christophe Destouches, Pascal Chaussonnet and Jean-Marc Laurens for their help in the experimental setup. We acknowledge the helpful comments of Roland Soule and the administrative support of our head of laboratory Philippe Fougeras. We are also grateful to the operating and maintenance teams of MASURCA. Finally, this work has benefited greatly from the many discussions with our foreign partners in the MUSE program.

REFERENCES

1. R. Soule, "The MUSE Experiments," In *Int. Conf. on Accelerator Driven Transmutation Technology and Applications*, Reno, Nevada, (2001).
2. G. M. Thomas, "Steady State Calculations in Support of the MUSE-4 Experimental Programme," In *This Conference*, Seoul, Korea, (2002).
3. P. Chaussonnet et al., *Cahier des charges fonctionnel "Système d'acquisition expérimental MASURCA"*, CEA - Cadarache (2002).
4. Y. Kitamura et al., "Reactor Noise Experiments by Using Acquisition System for Time Sries Data of Pulse Train," *J. Nucl. Sci. Technol.*, **36**[8], pp.653–660 (1999).
5. Y. Rugama et al., "Preliminary Measurements of the Prompt Neutron Decay Constant in MASURCA," In *SMORN VII: A Symposium on Bucl. Reactor Surveillance and Diagnostics*, Göteborg, Sweden, 27-31 May (2002).
6. D. Villamarín and E. González, "First CIEMAT measurements of the MUSE-4 kinetic response," In *This Conference*, Seoul, Korea, (2002).
7. R. P. Feynman et al., "Dispersion of The Neutron Emission In U-235 Fission," *J. Nucl. Energy*, **3**, pp.64–69 (1956).
8. K. O. Ott and R. J. Neuhold, *Introductory Nuclear Reactor Dynamics*, American Nuclear Society, (1985).
9. J. F. Lebrat, *Etude des incertitudes statistiques et systématiques sur les mesures de réactivité à MASURCA*, CEA - Cadarache (1997).
10. J. Durbin and G. Watson, "Testing for Serial Correlation in Least Squares Regression III," *Biometrika*, **58**, pp.1–19 (1971).
11. A. N. S. Institute, "U.S. Guide to the Expression of Uncertainty in Measurement," National Conference of Standards Laboratories (1997).
12. R. E. Uhrig, *Random Noise Techniques in Nuclear Reactor Systems*, Ronald Press, New York (1956).
13. G. I. Bell, "On the Stochastic Theory of Neutron Transport," *Nucl. Sci. Eng.*, **21**, pp.390– (1956).
14. Y. Yamane, "Feynman-α Formula with Dead Time Effect for a Symmetric Coupled-Core System," *Ann. Nucl. Energy*, **23**[12], pp.981 (1996).
15. S. K. Srinivasan and D. C. Sahni, "A Modified Statistical technique for the Measurement of α in Fast and Intermediate Reactor Assemblies," *Nucleonik*, **9**[3], pp.155–157 (1967).